

Compact dual-band double-negative metamaterial design based on the combination of electric and magnetic resonators

T. D. Karamanos, A. I. Dimitriadis, N. V. Kantartzis, and T. D. Tsiboukis

Department of Electrical and Computer Engineering, Aristotle University of Thessaloniki

GR-54124 Thessaloniki, Greece

Fax: +30 2310996312; email: tsibukis@auth.gr

Abstract

In this paper, the design of planar, double-negative metamaterials using electric and magnetic resonators is presented. The effective parameters of the proposed structures are extracted from the transmission and reflection coefficients by employing the Kramers-Kronig relations to solve the branch problem in the determination of the effective refractive index. Finally, the application of the proposed idea in the design of new multi-band, enhanced double-negative bandwidth or tunable metamaterials is explored.

1. Introduction

Since the first realization of a double-negative (DNG) metamaterial, various unit cell designs have been proposed to achieve a negative refraction medium [1-4]. Thin wires are usually utilized to provide negative effective permittivity, while magnetic resonators are selected to ensure negative permeability over the desired frequency band, leading to a DNG passband. However, the implementation of thin wires encounters significant practical issues, such as the reassurance of their contact with waveguide walls, the cross-cell intersections in isotropic metamaterials and their prohibitively thin dimensions for higher frequency problems.

Recently, electric ring resonators (ERRs) have been introduced for the design of epsilon-negative (ENG) metamaterials, as the electric equivalent of the SRRs [5]. These resonators possess an even number of conductive loops, due to their geometrical symmetry; hence their primary resonance is of electrical nature. Using the ERRs as an alternative to thin wires in the synthesis of DNG metamaterials offers feasible solutions to the aforementioned issues, whereas scalability can be exploited for applications virtually at every frequency range from microwave to visible. Furthermore, ERRs can be used as the basis for tunable materials.

In this paper, a novel compact DNG medium is developed, by imprinting ERRs and SRRs on both sides of a dielectric slab. The effective parameters of our configuration are extracted with the S -parameter retrieval technique, while the Kramers-Kronig relations are employed for uniquely determining the effective refractive index [6-9]. Finally, the proposed concept is extended in the design of a dual-band DNG metamaterial, to reveal its principal merits in designing advanced microwave components for various applications.

2. Design methodology for an ERR-SRR double-negative metamaterial

In order to obtain a DNG medium, two single-negative (SNG) materials are initially developed. A Taconic CER-10 substrate ($\epsilon_r = 10$, $\tan\delta = 0.0018$, thickness = 1.5 mm) is used as the host medium and unit cell dimensions are set to $z = 8$ mm, $y = 7.9$ mm, and $x = 7.5$ mm along the respective axes. All developed structures are excited by a plane wave propagating along the z -direction with its electric field toward y -axis.

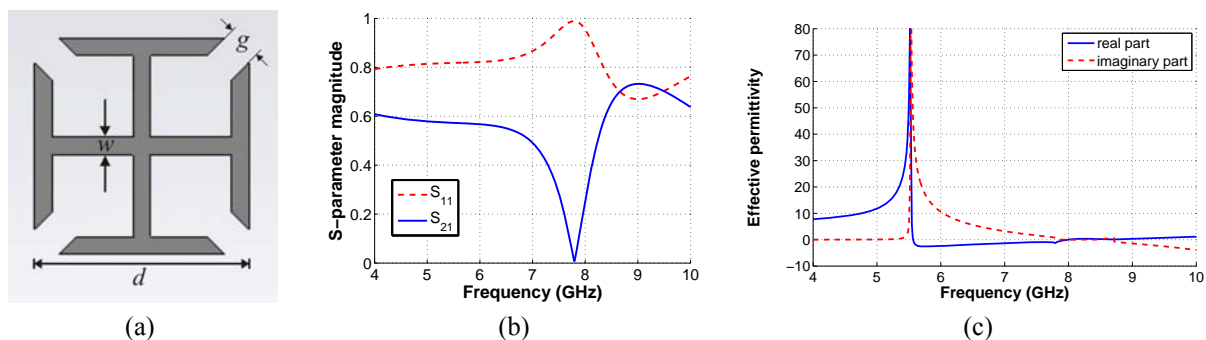


Fig. 1: (a) ERR geometry (dimensions: $d = 4.95$ mm, $g = 0.8$ mm, $w = 0.4$ mm), (b) magnitude of the S -parameters, and (c) effective permittivity. A stopband is observed around the design frequency of 7.8 GHz.

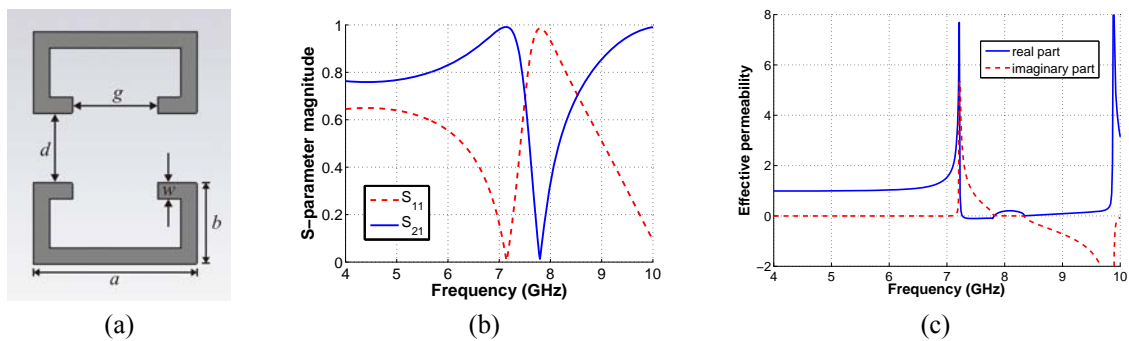


Fig. 2: (a) Axially-symmetric SRR geometry (dimensions: $a = 4$ mm, $b = 2$ mm, $g = 2$ mm, $d = 1.7$ mm, $w = 0.4$ mm), (b) magnitude of the S -parameters, and (c) effective permeability.

The ERR, shown in Fig. 1a, is selected to construct an ENG medium exhibiting a stopband with a center frequency of 7.8 GHz. To this objective, the $|S_{21}|$ minimum is shifted to that frequency by varying the structure's dimensions. The resulting ENG stopband and the respective negative permittivity are depicted in Figs 1b and 1c. On the other hand, a mu-negative (MNG) metamaterial is formed from the axially-symmetric SRR, as depicted in Fig. 2a. An optimization algorithm is applied to enforce the MNG region to overlap with that of the ENG material. From Figs 2b and 2c, it is observed that the MNG region is narrower than the ENG one, due to the attenuation of the SRR's magnetic resonance strength at higher frequencies.

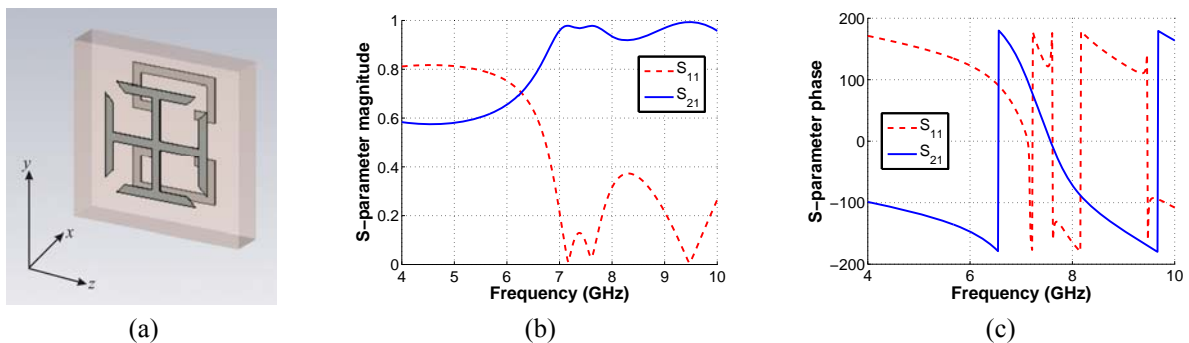


Fig. 3: (a) The ERR-SRR geometry, (b) magnitude of the S -parameters, and (c) phase of the S -parameters. The passband above 6.92 GHz is attributed to the double-negative behavior of the structure.

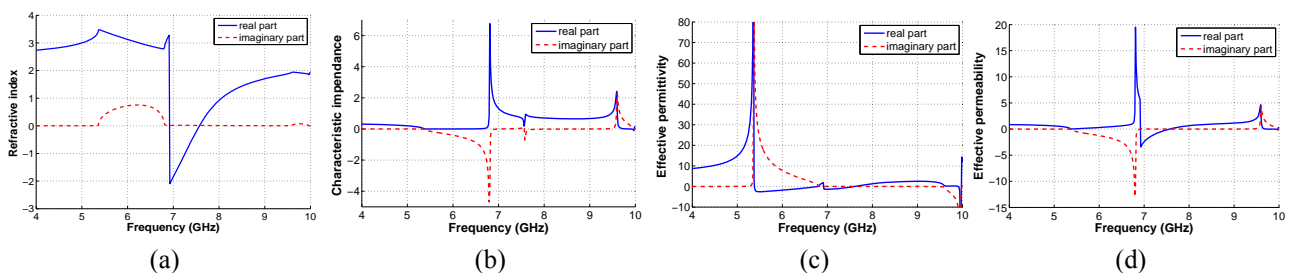


Fig. 4: Effective parameters: (a) refractive index n , (b) impedance z , (c) permittivity ϵ_r , and (d) permeability μ_r .

Afterwards, the previously designed SNG media are printed on both sides of the dielectric substrate, as in Fig. 3a. A closer inspection of Fig. 3b reveals a passband around the center frequency of 7 GHz. Also, the effective parameters of the medium have been extracted (Fig. 4). A negative refractive index is clearly obtained and the width of the DNG band is about 640 MHz. Interestingly, although the components have been designed for a resonant frequency of 7.8 GHz, the final DNG region begins approximately at 6.92 GHz. An explanation for this shift may stem from the parasitic inductances/capacitances that appear between the resonators due to their close proximity. These coupling effects remained relatively strong even when the substrate thickness was increased (not shown here), indicating that this is a side-effect of the structure's planar design.

3. Dual-band, negative-refraction medium

The previous design procedure can be employed for the synthesis of multi-band, enhanced negative-index bandwidth or even tunable metamaterials. In this section, a dual-band, negative-refraction medium is created by placing two different ERR-SRR unit cells adjacent to each other along the x -direction. Each unit

cell is designed for a different resonant frequency, by slightly varying the dimensions of its metallic parts, via the technique described in section 2. Due to the strong coupling between the two DNG components, their center frequencies and resonances' strengths are affected. Also, resonant frequencies other than the desired ones are likely to arise, owing to the Bloch modes, which gradually decrease when the intermediate space among the unit cells' metallic parts is enlarged. For this purpose, a dual-band DNG structure of enhanced performance by combining the ERR of Fig. 1a and the non-bianisotropic SRR, is presented in Fig. 5a. The individual SNG media have been designed for 7 and 8 GHz, whereas in the combined structure the negative index bands are slightly shifted downwards to 6.8 and 7.8 GHz, respectively. Finally, as a marginal case of a dual-band medium, a bandwidth-enhanced DNG medium may be formed, when the design frequencies of the unit cells come close enough to each other, so as to superimpose.

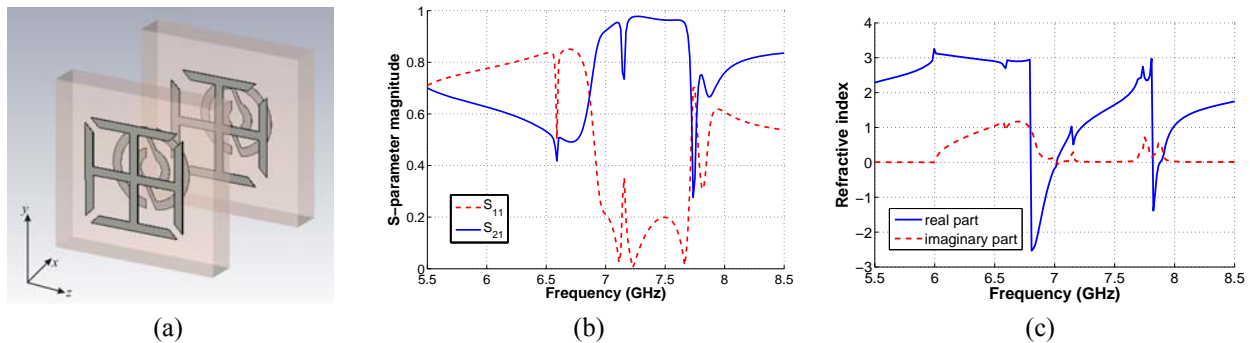


Fig. 5: (a) Dual-band DNG metamaterial unit cell geometry (dimensions: ERR1 for 7 GHz: $d = 4.94$ mm, $g = 0.4$ mm, $w = 0.4$ mm; NB-SRR1 for 7 GHz: $g = 0.5$ mm, $d = 0.6$ mm, $r = 1.93$ mm, $w = 0.4$ mm; ERR2 for 8 GHz: $d = 4.85$ mm, $g = 0.8$ mm, $w = 0.4$ mm; NB-SRR2 for 8 GHz: $g = 0.5$ mm, $d = 0.6$ mm, $r = 1.79$ mm, $w = 0.4$ mm), (b) S -parameters magnitude, and (c) effective refractive index n .

4. Conclusions

A new planar DNG metamaterial has been introduced in this paper via the combination of electric and magnetic resonators. The negative-refraction bandwidth of the structure has been found around 640 MHz, by applying an S -parameter-based homogenization method. It has to be stressed that for the unambiguous extraction of effective parameters, the Kramers-Kronig formulas have been implemented. By only slightly varying the resonators' dimensions, in order to shift their resonance frequency, and combining unit cells designed for different frequencies, multi-band, enhanced negative-index bandwidth or even tunable structures can be accomplished. The specific idea has been successfully illustrated in the realization of a dual-band metamaterial that can be utilized, among others, in the implementation of sub-wavelength cavity resonators and planar parallel plate waveguides.

References

- [1] J. B. Pendry, A. J. Holden, D. J. Robbins, and W. J. Stewart, Magnetism from conductors and enhanced nonlinear phenomena, *IEEE Trans. Microw. Theory Tech.*, vol. 47, no. 11, pp. 2075-2084, 1999.
- [2] F. Bilotti, A. Toscano, L. Vegni, K. Aydin, K. B. Alici, and E. Ozbay, Equivalent-circuit models for the design of metamaterials based on artificial magnetic inclusions, *IEEE Trans. Microw. Theory Tech.*, vol. 55, no. 12, pp. 2865-2873, 2007.
- [3] A. Alù, N. Engheta, A. Erentok, and R. W. Ziolkowski, Single-negative, double-negative, and low-index metamaterials and their electromagnetic applications, *IEEE Antennas Propag. Mag.*, vol. 49, no. 1, pp. 23-36, 2007.
- [4] R. Marqués, F. Martín, and M. Sorolla, Metamaterials with negative parameters: Theory, design and microwave applications, *Wiley-Interscience*, New Jersey, 2008.
- [5] H.-T. Chen, J. F. O'Hara, A. J. Taylor, R. D. Averitt, C. Highstrete, M. Lee, and W. J. Padilla, Complementary planar terahertz metamaterials, *Opt. Express*, vol. 15, no. 3, pp. 1084-1095, 2007.
- [6] X. Chen, T. M. Grzegorzczak, B.-I. Wu, J. Pacheco Jr., and J. A. Kong, Robust method to retrieve the constitutive parameters of metamaterials, *Phys. Rev. E*, vol. 70, p. 016608, 2004.
- [7] D. R. Smith, D. C. Vier, T. Koschny, and C. M. Soukoulis, Electromagnetic parameter retrieval from inhomogeneous metamaterials, *Phys. Rev. E*, vol. 71, p. 036617, 2005.
- [8] V. V. Varadan and R. Ro, Unique retrieval of complex permittivity and permeability of dispersive materials from reflection and transmitted fields by enforcing causality, *IEEE Trans. Microw. Theory Tech.*, vol. 55, no. 10, 2007.
- [9] A. B. Yakovlev, M. G. Silveirinha, O. Luukkonen, C. R. Simovski, I. S. Nefedov, and S. A. Tretyakov, Simple and efficient solution for mushroom surfaces – Local versus nonlocal homogenization, *Proc. Metamaterials'2010*, pp. 721-723, Karlsruhe, Germany, 2010.